MYOSTATIN-LIKE PROTEINS REGULATE SYNAPTIC FUNCTION AND NEURONAL MORPHOLOGY

Hrvoje Augustin[a,b], Kieran McGourty[c*], Joern R. Steinert[d*], Helena M. Cochemé[a,b,e,f], Jennifer Adcott[a,b], Melissa Cabecinha[a], Alec Vincent[a], Els F. Halff[g], Josef T. Kittler[g], Emmanuel Boucrot[c], Linda Partridge[a,b]

[a] Institute of Healthy Ageing, and GEE, University College London, Darwin Building, Gower Street, London WC1E 6BT, UK.

[b] Max Planck Institute for Biology of Ageing, Joseph-Stelzmann-Str. 9b, D50931 Cologne, Germany.

[c] Institute of Structural and Molecular Biology, University College London, Darwin Building Gower Street, London WC1E 6BT, UK.

[d] MRC Toxicology Unit, Hodgkin Building, University of Leicester, Lancaster Road, Leicester, LE1 9HN, UK.

[e] MRC Clinical Sciences Centre, Du Cane Road, London W12 0NN, UK.

[f] Institute of Clinical Sciences, Imperial College London, ICTEM Building, Hammersmith Hospital Campus, Du Cane Road, London W12 0NN, UK.

[g] Department of Neuroscience, Physiology and Pharmacology, University College London, Gower Street, London WC1E 6BT, UK.

[*] Equal contribution

ABSTRACT

Growth factors of the TGF-β superfamily play key roles in regulating neuronal and muscle function. Myostatin (or GDF8) and GDF11 are potent negative regulators of skeletal muscle mass. However, expression of both *Myostatin* and its cognate receptors in other tissues, including brain and peripheral nerves, suggests a potential wider biological role. Here, we show that Myoglianin (MYO), the *Drosophila* homolog of Myostatin and GDF11, regulates not only body weight and muscle size, but also inhibits neuromuscular synapse strength and composition in a Smad2-dependent manner. Both Myostatin and GDF11 affected synapse formation in isolated rat cortical neuron cultures, suggesting an effect on synaptogenesis beyond neuromuscular junctions. We also show that Myoglianin acts *in vivo* to inhibit synaptic transmission between neurons in the escape response neural circuit of adult flies. Thus, these anti-myogenic proteins act as important inhibitors of synapse function and neuronal growth.

INTRODUCTION

Organismal muscle mass is tightly regulated by positive and negative endocrine and autocrine/paracrine factors. Myostatin (also known as Growth and Differentiation Factor 8, or GDF8), a member of the transforming growth factor-ß (TGF-ß) superfamily of secreted differentiation and growth factors, is a potent inhibitor of skeletal muscle mass in mammals. *Myostatin* (*mst*) gene mutations or deletions cause hyperplastic and/or hypertrophic muscle growth in mice (McPherron et al., 1997) and a number of other species, including humans (Carnac et al., 2007), with consequent loss of muscle function (Gentry et al., 2011). Myostatin-like protein GDF11 (also known as BMP11) was also recently identified as a circulating inhibitor of skeletal muscle regeneration in rodents and, potentially, humans (Egerman et al., 2015).

Both GDF 8 and 11 bind to Activin-type receptor complexes, leading to the phosphorylation of intracellular Smad2/3 transcription factors, followed by their translocation to the nucleus (Oh et al., 2002; Rebbapragada et al., 2003). In addition to its action on muscles, GDF11 is a negative regulator of neuron number in the olfactory epithelium (Kawauchi et al., 2009; Wu et al., 2003), inhibitor of neuronal precursors giving rise to olfactory receptors (Gokoffski et al., 2011) and antagonist of neurogenesis during retinal development (Kim et al., 2005). *mst* transcript was recently detected in mouse brain (Lein et al., 2007) and Myostatin receptors are expressed in several tissues, including brain and peripheral nerves. Apart from a study demonstrating an inhibitory effect of Myostatin on neuronal colony formation in vitro (Wu et al., 2003), the potential role of Myostatin in the nervous system remains unexplored despite its potential biological and

therapeutic significance.

The *Drosophila myoglianin* (*myo*) gene encodes the invertebrate Activin-type ligand with the highest amino acid sequence homology to Myostatin and GDF11, both of which share 46% amino acid identity and >60% similarity with MYO (Lo and Frasch, 1999). Unlike the predominant *mst* expression in vertebrate skeletal muscle (Lee, 2004), *myo* is strongly expressed not only in different muscle types throughout development but also in embryonic (Lo and Frasch, 1999) and larval brain glia (Awasaki et al., 2011). Considering the strong expression of *GDF11* in the mammalian nervous system during development and adulthood (Nakashima et al., 1999; Shi and Liu, 2011), it is tempting to think of Myoglianin as combining the functions of Myostatin and GDF11 in flies.
In this study, we identified MYO as a strong inhibitor of synaptic function and composition at the larval NMJ, in addition to its role as an inhibitor of body weight and muscle size. These synaptic effects of MYO were mediated mainly by the transcription factor Smad2 (also known as Smox), and Shaggy, the Drosophila glycogen synthase kinase 3 (GSK-3) homolog. Myostatin could reverse the effect of MYO depletion on synaptic strength in larvae. Furthermore, Myostatin and GDF11 inhibited neuronal growth and synapse specification in rat cortical neurons, indicating that they can act directly on neurons that are not associated with muscle. The *in vivo* role of Myoglianin in regulating neuronal function was confirmed in a central, non-NMJ synapse in adult flies. Our findings show that Myoglianin and its mammalian orthologs Myostatin and GDF11 have previously unsuspected roles in the nervous system, acting as important inhibitors of synapse function and neuronal growth.

RESULTS

Myoglianin inhibits NMJ synapse strength and composition

The larval body wall musculature of *Drosophila* is composed of bilaterally symmetrical hemisegments, each consisting of 30 easily identifiable longitudinal and oblique multinucleated muscle cells/fibers. We focused on ventral longitudinal muscles 6 and 7 (Figure S1A), which are innervated by two axons forming a single glutamatergic neuromuscular junction (Ruiz-Canada and Budnik, 2006), a complex synapse composed of muscle, neuronal and glial cells.
We investigated the functional significance of the presence of MYO in larval musculature (Awasaki et al., 2011) electrophysiologically. We used microRNA (*miRNAmyo*) or dsRNA (*UAS-myoRNAi*) to down-regulate, and a *UAS-myoglianin* (WT) construct (Awasaki et al., 2011) to enhance *myo* expression by means of the *Mef2-GAL4* muscle driver (Brand and Perrimon, 1993; Ranganayakulu et al., 1995), resulting in *myo* expression changes in larval muscle preparations (Figure S1B).
Currents resulting from the spontaneous release of presynaptic vesicles (miniature excitatory

junctional currents (mEJCs), or “minis”) and evoked release (evoked excitatory junctional currents (eEJCs) represent two functional outputs at the neuromuscular synapse (Melom et al., 2013). Nerve-evoked postsynaptic currents, and the frequency of spontaneous release, reflect presynaptic, Ca^{2+}-dependent vesicular release (Peron et al., 2009), while mini amplitudes mainly reflect the postsynaptic sensitivity to transmitter, determined largely by the properties of glutamate receptors (DiAntonio et al., 1999). When eEJCs from muscle 6 were measured in the voltage-clamp mode (the membrane potential was clamped to -60 mV), we observed that experimentally reduced expression of *myo* in muscle increased eEJC amplitude, while over-expression reduced it (Figure 1A and 1B). While the mean mEJC frequency and amplitude remained unchanged across genotypes (Fig. S1C, D), the amplitude distribution showed a significant shift towards larger synaptic currents with *myo* knock-down in muscles (KS test, $P < 0.0001$) (Figure 1C and 1D), indicating increased post-synaptic sensitivity to glutamate. These data thus revealed that muscle-derived MYO is a potent suppressor of synaptic transmission at the NMJ through impact on both presynaptic release and postsynaptic sensitivity. On the postsynaptic side of the excitatory larval NMJ, heterotetrameric ionotropic glutamate receptors (GluRs) comprise two functionally distinct subtypes: IIA, containing the GluRIIA subunit, and IIB, containing the GluRIIB subunit, with IIA-type receptors generating larger synaptic currents and mediating functional strengthening of the NMJ (Petersen et al., 1997; Sigrist et al., 2002). Type IIB receptor subunits are characterized by faster desensitization kinetics and lower responsiveness to vesicularly released neurotransmitter (DiAntonio et al., 1999). Brp (Bruchpilot), a presynaptic marker, promotes active zone assembly and integrity, and vesicular neurotransmitter release (Kittel et al., 2006); the quantity of Brp has been associated with presynaptic strengthening at larval NMJ (Weyhersmuller et al., 2011). Prompted by our electrophysiological results, we measured the density of the GluRIIA receptor field, and the number of Brp puncta in the NMJ boutons (each bouton contains multiple active zones) (Figures 1E-1G). While *myo* levels negatively correlated with GluRIIA signal intensity (Figure 1G, *left*), only *myo* down-regulation (positively) affected the total active zone number (Figure S1E), and the number of Brp puncta normalized to the NMJ area (Figure 1G, *right*). This indicates that *myo* up-regulation and silencing affect presynaptic release through different mechanisms. To address the issue of potential off-target effects of the miRNA construct, we have confirmed our results by measuring the GluRIIA intensity in flies expressing an anti*myo* RNAi construct (Awasaki et al., 2011) in somatic muscles (Figure S1F). Myoglianin also negatively affects NMJ length and branching pattern (Figure S1G), in line with increased axonal branching in myostatin-null mice (Gay et al., 2012). The lack of effect on mini amplitudes in *myo* over-expressing animals despite the

reduction in IIA staining could be attributable to either compensatory increase in the levels of other GluR subunits present at the NMJ, or GluRIIA epitope masking (Renden and Broadie, 2003). We observed no effect of *myo* manipulations on the levels of IIB-type synaptic receptors (Figure S1H), indicating a receptor subtype-specific action of MYO. Together with our physiological data, these results demonstrate a significant inhibitory effect of muscle-derived MYO on the function and composition of the neuromuscular synapse.

Glia-expressed *myo* has a modulatory role at the NMJ

We next examined whether MYO was produced in the larval NMJ glia. We used a *UAS-GFP* construct driven by the *Myo-GAL4* driver (Awasaki et al., 2011), and detected a strong GFP-positive signal around synaptic boutons and in the extramuscular tracts running in parallel with the motoneurons innervating muscles 6 and 7 (green signal in Figure 2A). While the increased GFP signal intensity around boutons likely stems from the elaborate infoldings of the muscle membrane ensheathing the boutons called the subsynaptic reticulum, the extramuscular tracts (Figure 2A, arrowheads) imply glial *myo* expression at the larval NMJ, consistent with the previous detection of the *myo* transcript in peripheral larval glia (Fuentes-Medel et al., 2012). The effect of manipulation of *myo* expression in glia on synaptic physiology was less prominent than in muscle, probably because of the small size of the glial compartment at the NMJ in comparison with muscle, with only up-regulation reducing the mean evoked response amplitude (Figures 2B and 2C). We also observed a small, but significant (KS test, $P < 0.0001$), negative effect of glial *myo* on the distribution of miniature amplitudes (Figures 2D-2E), with the 'mini frequency' and mean 'mini amplitude' remaining unperturbed (Figures S2A and S2B). Knock-down of glial *myo* increased synaptic GluRIIA fluorescence (Figure S2C), consistent with the effect of *myo* knock-down on the distribution of mini amplitudes (Figures 2D-2E); we did not detect GluRIIA changes in *myo*-overexpressing animals, possibly due to relatively minor changes in receptor number and/or composition in these larvae (Figure S2C). Type-IIB receptor levels were unaffected by *myo* expression (Figure 2SD), and no significant effect of *myo* down-regulation was seen on the levels of type IIA receptors when *myo* was silenced in the motoneurons innervating larval body-wall muscles (Figure S2E), consistent with absence of MYO in this cell type. Together, these results imply a modulatory role for MYO of glial origin at the neuromuscular synapse.

Myoglianin displays a Myostatin-like effect on larval weight and muscle size

Having established a role for MYO at the NMJ, we next determined whether MYO resembles Myostatin in its negative impact on body weight, and adult (McPherron et al., 1997) and embryonic

(Manceau et al., 2008) muscle size. We first examined the effect of MYO on larval mass and muscle size. The wet weight of 3rd instar wandering larvae (72-96 h after hatching) was reduced by experimentally increased expression of *myo*, and increased by its knock-down, in larval muscle preparations (Figure 3A). Developmental progression (time to pupariation) was unaffected in these genotypes (Figure S3A). Wet weight was also increased in larvae expressing the previously used *myo* RNAi construct driven by a different muscle driver (*24B-GAL4*), and decreased in animals expressing an alternate *UAS-myoglianin* construct (see Experimental Procedures) (Figure S3B). Interestingly, we observed a similar effect on larval weight when *myo* constructs were driven with the pan-glial repo driver (Figure 3B). While miRNA against *myo* in motoneurons (Figure S3C) or fat body (Figure S3D) had no effect on larval weight, down-regulation of *myo* in the midgut resulted in significantly increased weight (Figure S3D), suggesting a role for Myoglianin outside the nervous system and muscle. Body wall muscles are the major constituent of the larval body in terms of size and mass (Bate et al., 1999), and we therefore examined the effect of *myo* expression on the size of the larval body-wall muscles 6 and 7 (Figure 3C). Similar to larval weight, the surface area of both muscles was reduced by increased *myo* expression, and increased by its knock-down, in the muscle (Figures 3D and S3E). We observed no difference between genotypes when *myo* expression was manipulated in glia (Figure 3E). Larval crawling speed was also negatively correlated with *myo* expression levels (Figure 3F, Supplemental movies 1-6), showing that manipulations of *myo* in muscle and glial cells have significant behavioural consequences. Together, these data establish a role for muscle-and glia-expressed *myo* as a strong negative regulator of larval weight and motility, and establish that muscle-derived MYO has a Myostatin-like function in regulating muscle size in *Drosophila* larvae.

Down-regulation of *myo* promotes signalling through GSK-3/Shaggy

We next identified potential intracellular mediators of reduced MYO, and their relevance for MYO action on synaptic physiology. Akt plays an important role in modulating synaptic plasticity in *Drosophila* (Guo and Zhong, 2006) and in mammals through phosphorylation-induced inhibition of GSK-3β (Peineau et al., 2007). We therefore investigated how manipulations of *myo* expression in muscles affected the levels of these signalling proteins in larval body-wall musculature. Down-regulation of *myo* significantly increased the levels of active, phosphorylated Akt (Figure S4A and S4B), with total Akt levels remaining stable across genotypes (Figure S4C), while phosphorylated Akt was unaffected by *myo* over-expression. While muscle-specific silencing of *myo* significantly increased the phosphorylation of GSK-3/Shaggy (Figures S4A and S4D), with up-regulation again having no effect, the levels of p-S6K, a marker for mTOR activation, were unperturbed by *myo*

manipulations (Figure S4E). We next wanted to examine the potential dependency of *myo* down-regulation on GSK-3/Shaggy and Akt in regulating synaptic physiology. Genetic *Akt* suppression in the muscle caused larval lethality in both control and "reduced MYO" background, precluding the investigation of genetic interactions between *myo* and *Akt*. RNAi-mediated down-regulation of GSK-3/Shaggy (*sggRNAi*), however, completely abolished the positive effect of *myo* silencing on the main electrophysiological parameters, eEJC (Figure S4F-G) and mEJC (KS test, $P < 0.0001$) (Figure S4H-I). Overall, these results implicate Shaggy as an intracellular effector of Myoglianin signalling at the larval NMJ synapse.

Smad2 mediates MYO signalling at the NMJ

The canonical model of TGF-β signalling in *Drosophila* assumes two possible intracellular mediators of MYO action: transcription factors MAD and Smad2 (Van der Zee et al., 2008). While the Activin-type ligands phosphorylate Smad2, BMP-like ligands in *Drosophila* work through transcription factor MAD (Fuentes-Medel et al., 2012; Peterson et al., 2012). If reduced MYO results in reduced MAD or Smad2 activity, then their forced activation should reverse the effects of MYO depletion. We expressed constitutively active forms of MAD or Smad2 in *myo* knock-down flies and measured evoked synaptic responses, the main readout for NMJ transmission strength. While activated MAD had no effect on evoked response in *Mef2GAL4/UAS-miRNAmyo* larvae, expression of the constitutively active Smad2 fully reversed the amplitude of the responses (Figure 4A and 4B). Activated Smad2 also completely (KS test, $P < 0.0001$) reversed the effect of supressed *myo* on the amplitude of spontaneous NMJ responses (Figure 4C). Activated MAD had a significant (KS test, $P < 0.019$) effect on the distribution of mEJCs (Figure 4A and 4C), but was unable to fully reverse the phenotype in *Mef2-GAL4/UAS-miRNAmyo* animals. We observed no effect of Smad2 or MAD activation on larval weight (Figure 4D), indicating that weight regulation by MYO requires alternative intracellular mediators. Smad2 is therefore a principal effector of MYO action on synaptic physiology in the larval NMJ.

Human Myostatin reverses the effects of *myo* silencing on synaptic strength in developing larvae

Genetic manipulations of *myo* only imply, but do not prove, a commensurate effect on the levels of MYO protein. We therefore conducted an experiment to establish whether human Myostatin protein could reverse the effects of *myo* knock-down. We injected either human Myostatin or control solution (BSA) into 2nd instar larvae 25-48 h after hatching; this juvenile stage is characterized by rapid tissue growth and peak larval protein synthesis rate (Church and Robertson, 1966). Importantly, both Myostatin and MYO have been shown to bind to the *Drosophila* TGF-β

(Wit/Babo) receptor complex (Lee-Hoeflich et al., 2005). If the effect of reduced *myo* expression on larval weight and/or synaptic physiology is mediated via reduced MYO synthesis and secretion, then extracellular injection of Myostatin should reverse these effects in 3rd instar wandering stage larvae. Injected Myostatin (~50 pg/larva, see Experimental Procedures) completely reversed the elevated mean eEJC response in *Mef2-GAL4/UAS-miRNAmyo* animals (Figure 5A and 5B); the postsynaptic density of type-IIA glutamate receptors was also reduced (Figure 5C and 5D) in these larvae, demonstrating the influence of Myostatin on both synaptic compartments. The inability of injected Myostatin to reverse the weight phenotype (Figure 5E) could be due to an insufficiently high Myostatin concentration acting on the somatic muscle tissue during larval growth. These results support the notion that the positive effect of *myo* silencing on synaptic composition and strength was due to reduced expression, synthesis and secretion of muscle-derived native MYO in developing larvae. They also suggest that Myostatin might regulate synaptic function in the mammalian nervous system.

Myostatin and GDF11 negatively affect synapse formation and neuronal morphology

The impact of *myo* mis-expression on synaptic composition at the NMJ cannot be unambiguously attributed to a direct action on neurons. We therefore tested whether physiological levels (10 ng/mL) (Chen et al., 2016; Lakshman et al., 2009; Schafer et al., 2016; Szulc et al., 2012) of mammalian MYO homologs Myostatin and GDF11 could modulate synaptogenesis in isolated mammalian neurons. Consistent with its role in synaptic development and plasticity (Caraci et al., 2015; Zhang et al., 1997), addition of TGFβ1 (5 ng/mL) (Czarkowska-Paczek et al., 2006; Ramesh et al., 1990) onto primary cortical rat neurons increased neurite outgrowth, reduced excitatory synapse formation and increased inhibitory synapse formation (Figure 6 and S5). This effect was likely mediated by Smad2/3 signalling, because inhibition of Alk5 (which composes the TGF-β receptor) with the small inhibitor A83-01 had the opposite effect, whereas direct activation of Smad2/3 with Alantolactone (bypassing the TGF-β receptor) mimicked TGF-β1 addition (Figure 6C-E and S5). As expected from its inhibition of neurogenesis (Nakashima et al., 2001), supraphysiological levels of BMP2 (10 ng/mL) (Fei et al., 2013) had the opposite effect, with a reduction in neurite outgrowth, increased excitatory synapse formation and reduced inhibitory synapse formation (Figure 6 and S5). Surprisingly, addition of Myostatin and GDF11 also reduced neurite outgrowth (Figure 6A-C), indicating that these two mammalian orthologs of *myo* do act directly on neurons and limit their capacity to connect with distant cells. This effect appears to be conserved across species, because *myo* down-regulation in larval muscles leads to an increased

number of neuron-to-muscle connections at the larval NMJ (Yu et al., 2013). Similar to TGF-β1, Myostatin and GDF11 signal through the Smad2/3 pathway (Oh et al., 2002; Rebbapragada et al., 2003). Interestingly, Myostatin reduced inhibitory synapse formation whereas GDF11 increased excitatory synapse formation (Figures 6), both affecting mainly the levels of pre-synaptic markers (Figure S5). Altogether, these finding show that Myostatin and GDF11 act directly on neurons by inhibiting neurite growth and modulating synaptogenesis.

Myoglianin inhibits a central synapse

To determine *in vivo* if MYO controls synapse function outside of the larval NMJ, we examined neurotransmission in the Giant Fiber System (GFS) of adult flies. This circuit mediates escape response by conveying visual and mechanosensory signals from the brain to the thoracic ganglia via two GF interneurons. The GFs activate the leg extensor muscle (TTM) via TTM motoneurons (TTMn) and electro-chemical GF-TTMn synapses; they also activate flight muscles (DLMs) by forming electrochemical connections with the peripherally synapsing interneuron (PSI), which in turn chemically synapses onto DLM motoneurons (DLMs) (Allen et al., 2006) (Figure 7A). Midline glia have been shown to promote GF-TTMn synapse formation during pupal development via Netrin-Frazzled signalling, and TTMn dendrites appear to physically contact the midline glia during development (Orr et al., 2014). We used the midline glia-specific *slit-GAL4* driver to manipulate *myo* in these cells during pupal development, and examined the effect on the GFS function in young adult flies, by measuring the latency between the stimulation of the GF cell bodies in the brain and TTM (or DLM) depolarization (Figure 7A). Silencing of *myo* had speeded up the transmission through the TTM (Figure 7B and 7C) but, as expected, not through the DLM (Figure S6) branch of the circuit, resulting in a mean response latency that is shorter than in the control genotype *(+/slit-GAL4*). Over-expression of *myo* had the opposite effect, lengthening the muscle response time following brain stimulation (Figure 7B and C). To assess a possible role of the NMJ between the TTMn and TTM, we stimulated the motoneuron directly by placing the stimulating electrodes in the thorax, thereby bypassing the GF axon (Figure 7A). The response latencies measured this way were normal (~0.6 ms) (Tanouye and Wyman, 1980) and did not differ between the genotypes (Figure 7D), implying no effect of MYO of midline glial origin on this NMJ. These data firmly implicate MYO in the formation of functional GF-TTMn synapses during adult development. Together, our results show that MYO is an *in vivo* inhibitor of synaptic transmission between neurons.

DISCUSSION

Growth factors regulate many aspects of tissue development, growth and metabolism. Myostatin and GDF11 are highly homologous members of the TGF-β superfamily of growth factors. While GDF11 plays a role in a variety of systems, the role of Myostatin appears to be confined to skeletal and cardiac muscles (Huang et al., 2011; Lee, 2004).

MYO is a negative regulator of synaptic transmission, larval weight and muscle size

Despite the previously described roles of MYO in neural remodelling and synapse refinement (Awasaki et al., 2011; Yu et al., 2013) very little is known about the impact of Myoglianin on synaptic physiology. We first established muscle-derived MYO as a negative regulator of both spontaneous and evoked response at the NMJ, demonstrating its role as a broad regulator of synaptic transmission. The highly coordinated apposition of active zones and glutamate receptors underlies their ability to regulate synaptic strength and plasticity of the larval NMJ (Marrus and DiAntonio, 2004). We show that muscle expression of *myo* inversely affects the NMJ quantity of Brp and GluRIIA, critical pre-and post-synaptic proteins, and determinants of evoked neurotransmitter release and quantal size (i.e. postsynaptic sensitivity to presynaptically released transmitter), respectively (DiAntonio et al., 1999; Kittel et al., 2006). While it is possible that MYO exerts its influence on synaptic strength through other mediators, GluRIIA and Brp are their likely downstream effectors. Our electrophysiological results, obtained using the *GAL4-UAS* system for targeted manipulation of *myo*, differ from the ones obtained recently using a genetic null *myo* mutant showing slightly reduced miniature amplitudes (Kim and O'Connor, 2014). The likely explanation is that compensatory effects happen in other tissues in the tissue-specific knockdown animals that cannot occur in genetic nulls, especially for systemic type factors. The other possible explanation is differential cross regulation between different (MYO-like) ligands in genetic null *vs* tissue knockdown animals. These results thus indicate the relevance of tissue specificity of MYO action, and of *myo* expression levels, in regulating synaptic function, and emphasize the need for caution when interpreting results from different types of gene manipulations.

We detected *myo* expression in the glial cells of the larval neuromuscular junction. While *Drosophila* NMJ contains at least 2 subtypes of glia (Augustin et al., 2007), *myo* expression appears confined to the ‘repo-positive’ subtype both in the central (Awasaki et al., 2011) and peripheral nervous system (this work). The dual muscle and glial presence makes MYO ideally positioned for regulating NMJ function. Due to the small size of the compartment, however, glia-derived MYO likely has a modulatory role at the neuromuscular junction.

We have also found that muscle suppression of Myoglianin, a *Drosophila* homolog of Myostatin

and GDF11, promotes increased larval weight and body-wall muscle size in developing larvae, resembling the effect of *Myostatin* knockdown in mammals. Interestingly, pan-glial expression of *myo* negatively affected larval wet weight, but not the size of somatic myofibers, suggesting previously unsuspected systemic roles for glial cells.

Smad2 is a downstream effector of MYO

We found that Smad2 is a mediator of MYO action on both evoked response and postsynaptic sensitivity, with MAD having a minor effect on the latter. While MAD primarily functions as a cytoplasmic transducer of BMP signalling, it has been demonstrated that, under certain conditions, MAD can be phosphorylated in response to Activin pathway activation (Peterson et al., 2012). We have detected elevated levels of phosphorylated Akt and GSK-3/Shaggy in larval somatic muscles of animals with reduced *myo* expression in this tissue. In flies and mammals, the Akt-mTOR axis promotes skeletal muscle growth (Piccirillo et al., 2014), and phosphorylation-induced inhibition of GSK-3/Shaggy induces hypertrophy in skeletal myotube (Vyas et al., 2002). The effects of attenuated *myo* expression on larval tissue size, however, do not appear to be mediated by Smad2 (or MAD) activation as their overexpression does not reverse the weight phenotype in "low *myo*" background. Indeed, "non-Smad" signalling pathways have been demonstrated for various TGF-β ligands in vertebrates and *Drosophila* (Huang et al., 2011; Ng, 2008). In addition to its role as an inhibitor of the NMJ growth (Franco et al., 2004) and active zone formation (Viquez et al., 2009) in developing *Drosophila* larvae, GSK-3β is also a critical promoter of synaptic plasticity (Nelson et al., 2013; Peineau et al., 2009; Peineau et al., 2007), possibly through regulation of glutamate receptor function or trafficking (Bradley et al., 2012; Salcedo-Tello et al., 2011; Wei et al., 2010). Our work has revealed Shaggy as a mediator of reduced MYO action, and as a negative regulator of synaptic strength at the larval NMJ. While MYO likely affects both sides of the synapse directly, an unlikely but possible scenario is that presynaptic motoneuron responds to a retrograde signal released from muscle/glial cells at the NMJ in response to an induction by MYO. An attractive hypothesis is that MYO negatively regulates presynaptic release directly, in conjunction with muscle-secreted Gbb, a positive regulator of neuromuscular synapse development and growth (McCabe et al., 2003). The effects of MYO could also be mediated through the transmembrane protein Plum, previously proposed to regulate connectivity at the larval NMJ by sequestrating Myoglianin (Yu et al., 2013).

Myostatin negatively regulates synaptic function and neuronal morphology

We found that injections of Myostatin into rapidly growing larvae abolish the positive effect of *myo* down-regulation on NMJ strength and composition, and reverse the elevated muscle p-Akt levels.

Furthermore, both Myostatin and GDF11 supressed the growth of neuronal processes and perturbed the formation of synapses in cultured brain neurons, suggesting a direct action on neurons and regulation of synaptogenesis beyond neuromuscular junctions. Recently, Myostatin transcript and protein were detected in the mouse hippocampus and olfactory system neurons, respectively (Iwasaki et al., 2013; Lein et al., 2007), and Myostatin type I (Alk4/5) and type II (ActIIB) receptors were found to be expressed in the mammalian nervous system (Bottner et al., 1996; Cameron et al., 1994; Rebbapragada et al., 2003). Our results therefore expand on these findings, suggesting functional relevance for Myostatin in both peripheral and central nervous system, and beyond its action as a canonical regulator of skeletal muscle growth. These novel roles remain to be further explored.

Myoglianin is a broad regulator of synaptic function in flies

We have expanded our analysis of the functional relevance of MYO in the nervous system by demonstrating its importance in a non-NMJ synapse. Specifically, Myoglianin plays a role in the development of a mixed electro-chemical synapse in the *Drosophila* escape response pathway, likely by regulating the density of *shakB*-encoded gap junctions at the GF-TTMn synapse (Blagburn et al., 1999). These findings implicate MYO as a broad negative regulator of neuronal function across the nervous system and developmental stages.

Our work thus reveals broad and novel roles for anti-myogenic TGF-β superfamily of proteins in the nervous system and suggests new targets for interventions into synaptic function across species.

MATERIALS AND METHODS

Drosophila experiments

Fly stocks and husbandry

All stocks were maintained and all experiments were conducted at 25ºC on a 12 h:12 h light:dark cycle at constant humidity using standard sugar/yeast/agar (SYA) media (15g/l agar, 50 g/l sugar, 100 g/l autolysed yeast, 100g/l nipagin and 3ml/l propionic acid) (Bass et al., 2007). 2nd and 3rd instar larvae used in the experiments were selected based on morphological (larval spiracles and mouth-hook) and behavioural criteria. Flies were mated for 48 h before separating females from males. *Drosophila* stocks used in the paper are described in Supplemental Experimental Procedures.

Larval NMJ electrophysiology

Recordings were performed as previously described (Robinson et al., 2014). TEVC recordings using sharp-electrodes were made from ventral longitudinal muscle 6 in abdominal segments 2 and 3 of 3rd instar larvae.

GFS electrophysiology

Recordings from the Giant Fiber system were done as described previously (Allen et al., 1999; Augustin et al., 2011).

Immunocytochemistry and confocal microscopy

Immunocytochemistry and confocal microscopy were performed as described previously (Augustin et al., 2007) using Zeiss 700 inverted confocal microscope. All neuromuscular junction (NMJ) images and analyses were from NMJs on larval ventral longitudinal muscles 6 and 7 (hemisegments A3–A4). Measurements of the density of postsynaptic glutamate receptors were made using ImageJ by drawing a circle around quantifying mean postsynaptic immunofluorescence intensity relative to fluorescence in surrounding muscle tissue ($F_{synapse}$-$F_{background}$ membrane). Brp densities were calculated by counting the number of Brp puncta per NMJ and dividing by the area of the pre-synaptic motor neuron.

Western blots

Larval muscle preps were dissected (6 preps per sample, 3-5 samples per genotype per experiment) in cold HL3 buffer and flash frozen prior to western blot analysis.

Cell culture experiments

Synapse labelling, image processing and quantitation

Neuronal cell cultures were prepared and treated as outlined in more detail in supplementary methods, after which cells were fixed in 4% paraformaldehyde (PFA), permeabilized with 0.1% Triton-PBS and labelled using DAPI, anti-MAP2 and either anti-vGLUT1 and anti-PSD95 or anti-Gephyrin and anti-VGAT. Images of labelled cells were acquired using a high-content analysis system (ImageXpress, Micro XLS, Molecular Devices). Image analysis was performed using a protocol established in CellProfiler image analysis software (Kamentsky et al., 2011) and is a variation on a protocol established previously (Nieland et al., 2014). A set of image analysis algorithms or 'pipeline' was constructed to measure the properties of interest within the cortical neuron culture labelled with either DAPI, anti-MAP2, anti-PSD95 and antivGLUT1 or with DAPI, anti-MAP2, anti-Gephyrin and anti-VGAT. Each image-set, corresponding to one field of view or site

and comprising four fluorescently labelled channels, were analysed independently using this pipeline. 9 sites per well were analysed and repeated in triplicate experiments. Refer to supplementary data for further details on the statistical analysis, experimental procedures and reagents used.

ACKNOWLEDGEMENTS

We would like to thank Michael O'Connor (University of Minnesota, USA) for myoglianin lines, useful discussions and comments on the manuscript, Takeshi Awasaki (Janelia Farm, USA, and Kyorin University, Japan) for myoglianin miRNA lines, as well as the Bloomington Drosophila Stock Center for reagents.

COMPETING INTERESTS

The authors declare no competing or financial interests.

AUTHOR CONTRIBUTIONS

H.A. and L.P. designed the study, E.B designed tissue culture experiments, H.A., K.M., J.R.S., J.A., H.M.C., M.C., and A.V. conducted experiments, H.A., J.S., and K.M. analysed the data, E.F.H. and J.T.K. provided neuronal cells, H.A. and L.P. wrote the manuscript with a significant input from E.B. and K.M. All authors discussed the results and reviewed the manuscript.

FUNDING

This work was funded by a Wellcome Trust Strategic Award to L.P., the Max Planck Society and a Biotechnology and Biological Sciences Research Council David Phillips fellowship (to EB)

REFERENCES

Allen, M. J., Godenschwege, T. A., Tanouye, M. A. and Phelan, P. (2006). Making an escape: development and function of the Drosophila giant fibre system. *Semin Cell Dev Biol* **17**, 31-41.

Allen, M. J., Shan, X., Caruccio, P., Froggett, S. J., Moffat, K. G. and Murphey, R. K. (1999). Targeted expression of truncated glued disrupts giant fiber synapse formation in Drosophila. *The Journal of neuroscience : the official journal of the Society for Neuroscience* **19**, 9374-9384.

Augustin, H., Allen, M. J. and Partridge, L. (2011). Electrophysiological recordings from the giant fiber pathway of D. melanogaster. *J Vis Exp*.

Augustin, H., Grosjean, Y., Chen, K., Sheng, Q. and Featherstone, D. E. (2007). Nonvesicular release of glutamate by glial xCT transporters suppresses glutamate receptor clustering in vivo. *The Journal of neuroscience : the official journal of the Society for Neuroscience* **27**, 111-123.

Awasaki, T., Huang, Y., O'Connor, M. B. and Lee, T. (2011). Glia instruct developmental neuronal remodeling through TGF-beta signaling. *Nature neuroscience* **14**, 821-823.

Bass, T. M., Grandison, R. C., Wong, R., Martinez, P., Partridge, L. and Piper, M. D. (2007). Optimization of dietary restriction protocols in Drosophila. *J Gerontol A Biol Sci Med Sci* **62**, 1071-1081.

Bate, M., Landgraf, M. and Ruiz Gomez Bate, M. (1999). Development of larval body wall muscles. *Int Rev Neurobiol* **43**, 25-44.

Blagburn, J. M., Alexopoulos, H., Davies, J. A. and Bacon, J. P. (1999). Null mutation in shaking-B eliminates electrical, but not chemical, synapses in the Drosophila giant fiber system: a structural study. *J Comp Neurol* **404**, 449-458.

Bottner, M., Unsicker, K. and Suter-Crazzolara, C. (1996). Expression of TGF-beta type II receptor mRNA in the CNS. *Neuroreport* **7**, 2903-2907.

Bradley, C. A., Peineau, S., Taghibiglou, C., Nicolas, C. S., Whitcomb, D. J., Bortolotto, Z. A., Kaang, B. K., Cho, K., Wang, Y. T. and Collingridge, G. L. (2012). A pivotal role of GSK-3 in synaptic plasticity. *Front Mol Neurosci* **5**, 13.

Brand, A. H. and Perrimon, N. (1993). Targeted gene expression as a means of altering cell fates and generating dominant phenotypes. *Development* **118**, 401-415.

Cameron, V. A., Nishimura, E., Mathews, L. S., Lewis, K. A., Sawchenko, P. E. and Vale, W. W. (1994). Hybridization histochemical localization of activin receptor subtypes in rat brain, pituitary, ovary, and testis. *Endocrinology* **134**, 799-808.

Caraci, F., Gulisano, W., Guida, C. A., Impellizzeri, A. A., Drago, F., Puzzo, D. and Palmeri, A. (2015). A key role for TGF-beta1 in hippocampal synaptic plasticity and memory. *Sci Rep* **5**, 11252.

Carnac, G., Vernus, B. and Bonnieu, A. (2007). Myostatin in the pathophysiology of skeletal muscle. *Current genomics* **8**, 415-422.

Chen, Y., Guo, Q., Zhang, M., Song, S., Quan, T., Zhao, T., Li, H., Guo, L., Jiang, T. and Wang, G. (2016). Relationship of serum GDF11 levels with bone mineral density and bone turnover markers in postmenopausal Chinese women. *Bone Res* **4**, 16012.

Church, R. B. and Robertson, F. W. (1966). A biochemical study of the growth of Drosophila melanogaster. . *J Exp Zool* **162**, 337-351.

Czarkowska-Paczek, B., Bartlomiejczyk, I. and Przybylski, J. (2006). The serum levels of growth factors: PDGF, TGF-beta and VEGF are increased after strenuous physical exercise. *J Physiol Pharmacol* **57**, 189-197.

DiAntonio, A., Petersen, S. A., Heckmann, M. and Goodman, C. S. (1999). Glutamate receptor expression regulates quantal size and quantal content at the Drosophila neuromuscular junction. *The Journal of neuroscience : the official journal of the Society for Neuroscience* **19**, 3023-3032.

Egerman, M. A., Cadena, S. M., Gilbert, J. A., Meyer, A., Nelson, H. N., Swalley, S. E., Mallozzi, C., Jacobi, C., Jennings, L. L., Clay, I., et al. (2015). GDF11 Increases with Age and Inhibits Skeletal Muscle Regeneration. *Cell Metab* **22**, 164-174.

Fei, Z. H., Yao, C. Y., Yang, X. L., Huang, X. E. and Ma, S. L. (2013). Serum BMP-2 up-regulation as an indicator of poor survival in advanced non-small cell lung cancer patients. *Asian Pac J Cancer Prev* **14**, 5293-5299.

Franco, B., Bogdanik, L., Bobinnec, Y., Debec, A., Bockaert, J., Parmentier, M. L. and Grau, Y. (2004). Shaggy, the homolog of glycogen synthase kinase 3, controls neuromuscular junction growth in Drosophila. *The Journal of neuroscience : the official journal of the Society for Neuroscience* **24**, 6573-6577.

Fuentes-Medel, Y., Ashley, J., Barria, R., Maloney, R., Freeman, M. and Budnik, V. (2012). Integration of a retrograde signal during synapse formation by glia-secreted TGF-beta ligand. *Current biology : CB* **22**, 1831-1838.

Gay, S., Jublanc, E., Bonnieu, A. and Bacou, F. (2012). Myostatin deficiency is associated with an increase in number of total axons and motor axons innervating mouse tibialis anterior muscle. *Muscle & nerve* **45**, 698-704.

Gentry, B. A., Ferreira, J. A., Phillips, C. L. and Brown, M. (2011). Hindlimb skeletal muscle function in myostatin-deficient mice. *Muscle & nerve* **43**, 49-57.

Gokoffski, K. K., Wu, H. H., Beites, C. L., Kim, J., Kim, E. J., Matzuk, M. M., Johnson, J. E., Lander, A. D. and Calof, A. L. (2011). Activin and GDF11 collaborate in feedback control of neuroepithelial stem cell proliferation and fate. *Development* **138**, 4131-4142.

Guo, H. F. and Zhong, Y. (2006). Requirement of Akt to mediate long-term synaptic depression in Drosophila. *The Journal of neuroscience : the official journal of the Society for Neuroscience* **26**, 4004-4014.

Huang, Z., Chen, X. and Chen, D. (2011). Myostatin: a novel insight into its role in metabolism, signal pathways, and expression regulation. *Cellular signalling* **23**, 1441-1446.

Iwasaki, S., Miyake, M., Watanabe, H., Kitagawa, E., Watanabe, K., Ohwada, S., Kitazawa, H., Rose, M. T. and Aso, H. (2013). Expression of myostatin in neural cells of the olfactory system. *Mol Neurobiol* **47**, 1-8.

Kamentsky, L., Jones, T. R., Fraser, A., Bray, M. A., Logan, D. J., Madden, K. L., Ljosa, V., Rueden, C., Eliceiri, K. W. and Carpenter, A. E. (2011). Improved structure, function and compatibility for CellProfiler: modular high-throughput image analysis software. *Bioinformatics* **27**, 1179-1180.

Kawauchi, S., Kim, J., Santos, R., Wu, H. H., Lander, A. D. and Calof, A. L. (2009). Foxg1 promotes olfactory neurogenesis by antagonizing Gdf11. *Development* **136**, 1453-1464.

Kim, J., Wu, H. H., Lander, A. D., Lyons, K. M., Matzuk, M. M. and Calof, A. L. (2005). GDF11 controls the timing of progenitor cell competence in developing retina. *Science* **308**, 1927-1930.

Kim, M. J. and O'Connor, M. B. (2014). Anterograde Activin signaling regulates postsynaptic membrane potential and GluRIIA/B abundance at the Drosophila neuromuscular junction. *PloS one* **9**, e107443.

Kittel, R. J., Wichmann, C., Rasse, T. M., Fouquet, W., Schmidt, M., Schmid, A., Wagh, D. A., Pawlu, C., Kellner, R. R., Willig, K. I., et al. (2006). Bruchpilot promotes active zone assembly, Ca2+ channel clustering, and vesicle release. *Science* **312**, 1051-1054.

Lakshman, K. M., Bhasin, S., Corcoran, C., Collins-Racie, L. A., Tchistiakova, L., Forlow, S. B., St Ledger, K., Burczynski, M. E., Dorner, A. J. and Lavallie, E. R. (2009). Measurement of myostatin concentrations in human serum: Circulating concentrations in young and older men and effects of testosterone administration. *Mol Cell Endocrinol* **302**, 26-32.

Lee-Hoeflich, S. T., Zhao, X., Mehra, A. and Attisano, L. (2005). The Drosophila type II receptor, Wishful thinking, binds BMP and myoglianin to activate multiple TGFbeta family signaling pathways. *FEBS letters* **579**, 4615-4621.

Lee, S. J. (2004). Regulation of muscle mass by myostatin. *Annual review of cell and developmental biology* **20**, 61-86.

Lein, E. S., Hawrylycz, M. J., Ao, N., Ayres, M., Bensinger, A., Bernard, A., Boe, A. F., Boguski, M. S., Brockway, K. S., Byrnes, E. J., et al. (2007). Genome-wide atlas of gene expression in the adult mouse brain. *Nature* **445**, 168-176.

Lo, P. C. and Frasch, M. (1999). Sequence and expression of myoglianin, a novel Drosophila gene of the TGF-beta superfamily. *Mechanisms of development* **86**, 171-175.

Manceau, M., Gros, J., Savage, K., Thome, V., McPherron, A., Paterson, B. and Marcelle, C. (2008). Myostatin promotes the terminal differentiation of embryonic muscle progenitors. *Genes & development* **22**, 668-681.

Marrus, S. B. and DiAntonio, A. (2004). Preferential localization of glutamate receptors opposite sites of high presynaptic release. *Current biology : CB* **14**, 924-931.

McCabe, B. D., Marques, G., Haghighi, A. P., Fetter, R. D., Crotty, M. L., Haerry, T. E., Goodman, C. S. and O'Connor, M. B. (2003). The BMP homolog Gbb provides a retrograde signal that regulates synaptic growth at the Drosophila neuromuscular junction. *Neuron* **39**, 241-254.

McPherron, A. C., Lawler, A. M. and Lee, S. J. (1997). Regulation of skeletal muscle mass in mice by a new TGF-beta superfamily member. *Nature* **387**, 83-90.

Melom, J. E., Akbergenova, Y., Gavornik, J. P. and Littleton, J. T. (2013). Spontaneous and evoked release are independently regulated at individual active zones. *The Journal of neuroscience : the official journal of the Society for Neuroscience* **33**, 17253-17263.

Nakashima, K., Takizawa, T., Ochiai, W., Yanagisawa, M., Hisatsune, T., Nakafuku, M., Miyazono, K., Kishimoto, T., Kageyama, R. and Taga, T. (2001). BMP2-mediated alteration in the developmental pathway of fetal mouse brain cells from neurogenesis to astrocytogenesis. *Proc Natl Acad Sci U S A* **98**, 5868-5873.

Nakashima, M., Toyono, T., Akamine, A. and Joyner, A. (1999). Expression of growth/differentiation factor 11, a new member of the BMP/TGFbeta superfamily during mouse embryogenesis. *Mechanisms of development* **80**, 185-189.

Nelson, C. D., Kim, M. J., Hsin, H., Chen, Y. and Sheng, M. (2013). Phosphorylation of threonine-19 of PSD-95 by GSK-3beta is required for PSD-95 mobilization and long-term depression. *The Journal of neuroscience : the official journal of the Society for Neuroscience* **33**, 12122-12135.

Ng, J. (2008). TGF-beta signals regulate axonal development through distinct Smad-independent mechanisms. *Development* **135**, 4025-4035.

Nieland, T. J., Logan, D. J., Saulnier, J., Lam, D., Johnson, C., Root, D. E., Carpenter, A. E. and Sabatini, B. L. (2014). High content image analysis identifies novel regulators of synaptogenesis in a high-throughput RNAi screen of primary neurons. *PloS one* **9**, e91744.

Oh, S. P., Yeo, C. Y., Lee, Y., Schrewe, H., Whitman, M. and Li, E. (2002). Activin type IIA and IIB receptors mediate Gdf11 signaling in axial vertebral patterning. *Genes & development* **16**, 2749-2754.

Orr, B. O., Borgen, M. A., Caruccio, P. M. and Murphey, R. K. (2014). Netrin and Frazzled regulate presynaptic gap junctions at a Drosophila giant synapse. *The Journal of neuroscience : the official journal of the Society for Neuroscience* **34**, 5416-5430.

Peineau, S., Nicolas, C. S., Bortolotto, Z. A., Bhat, R. V., Ryves, W. J., Harwood, A. J., Dournaud, P., Fitzjohn, S. M. and Collingridge, G. L. (2009). A systematic investigation of the protein kinases involved in NMDA receptor-dependent LTD: evidence for a role of GSK-3 but not other serine/threonine kinases. *Mol Brain* **2**, 22.

Peineau, S., Taghibiglou, C., Bradley, C., Wong, T. P., Liu, L., Lu, J., Lo, E., Wu, D., Saule, E., Bouschet, T., et al. (2007). LTP inhibits LTD in the hippocampus via regulation of GSK3beta. *Neuron* **53**, 703-717.

Peron, S., Zordan, M. A., Magnabosco, A., Reggiani, C. and Megighian, A. (2009). From action potential to contraction: neural control and excitation-contraction coupling in larval muscles of Drosophila. *Comparative biochemistry and physiology. Part A, Molecular & integrative physiology* **154**, 173-183.

Petersen, S. A., Fetter, R. D., Noordermeer, J. N., Goodman, C. S. and DiAntonio, A. (1997). Genetic analysis of glutamate receptors in Drosophila reveals a retrograde signal regulating presynaptic transmitter release. *Neuron* **19**, 1237-1248.

Peterson, A. J., Jensen, P. A., Shimell, M., Stefancsik, R., Wijayatonge, R., Herder, R., Raftery, L. A. and O'Connor, M. B. (2012). R-Smad competition controls activin receptor output in Drosophila. *PloS one* **7**, e36548.

Piccirillo, R., Demontis, F., Perrimon, N. and Goldberg, A. L. (2014). Mechanisms of muscle growth and atrophy in mammals and Drosophila. *Dev Dyn* **243**, 201-215.

Ramesh, C., Pohl, R., Balon, R. and Yeragani, V. K. (1990). Effect of imipramine on liver function tests. *Pharmacopsychiatry* **23**, 56-57.

Ranganayakulu, G., Zhao, B., Dokidis, A., Molkentin, J. D., Olson, E. N. and Schulz, R. A. (1995). A series of mutations in the D-MEF2 transcription factor reveal multiple functions in larval and adult myogenesis in Drosophila. *Developmental biology* **171**, 169-181.

Rebbapragada, A., Benchabane, H., Wrana, J. L., Celeste, A. J. and Attisano, L. (2003). Myostatin signals through a transforming growth factor beta-like signaling pathway to block adipogenesis. *Mol Cell Biol* **23**, 7230-7242.

Renden, R. B. and Broadie, K. (2003). Mutation and activation of Galpha s similarly alters pre- and postsynaptic mechanisms modulating neurotransmission. *J Neurophysiol* **89**, 2620-2638.

Robinson, S. W., Nugent, M. L., Dinsdale, D. and Steinert, J. R. (2014). Prion protein facilitates synaptic vesicle release by enhancing release probability. *Human molecular genetics*.

Ruiz-Canada, C. and Budnik, V. (2006). Introduction on the use of the Drosophila embryonic/larval neuromuscular junction as a model system to study synapse development and function, and a brief summary of pathfinding and target recognition. *Int Rev Neurobiol* **75**, 1-31.

Salcedo-Tello, P., Ortiz-Matamoros, A. and Arias, C. (2011). GSK3 Function in the Brain during Development, Neuronal Plasticity, and Neurodegeneration. *Int J Alzheimers Dis* **2011**, 189728.

Schafer, M. J., Atkinson, E. J., Vanderboom, P. M., Kotajarvi, B., White, T. A., Moore, M. M., Bruce, C. J., Greason, K. L., Suri, R. M., Khosla, S., et al. (2016). Quantification of GDF11 and Myostatin in Human Aging and Cardiovascular Disease. *Cell Metab* **23**, 1207-1215.

Shi, Y. and Liu, J. P. (2011). Gdf11 facilitates temporal progression of neurogenesis in the developing spinal cord. *The Journal of neuroscience : the official journal of the Society for Neuroscience* **31**, 883-893.

Sigrist, S. J., Thiel, P. R., Reiff, D. F. and Schuster, C. M. (2002). The postsynaptic glutamate receptor subunit DGluR-IIA mediates long-term plasticity in Drosophila. *The Journal of neuroscience : the official journal of the Society for Neuroscience* **22**, 7362-7372.

Szulc, P., Schoppet, M., Goettsch, C., Rauner, M., Dschietzig, T., Chapurlat, R. and Hofbauer, L. C. (2012). Endocrine and clinical correlates of myostatin serum concentration in men--the STRAMBO study. *J Clin Endocrinol Metab* **97**, 3700-3708.

Tanouye, M. A. and Wyman, R. J. (1980). Motor outputs of giant nerve fiber in Drosophila. *J Neurophysiol* **44**, 405-421.

Van der Zee, M., da Fonseca, R. N. and Roth, S. (2008). TGFbeta signaling in Tribolium: vertebrate-like components in a beetle. *Dev Genes Evol* **218**, 203-213.

Viquez, N. M., Fuger, P., Valakh, V., Daniels, R. W., Rasse, T. M. and DiAntonio, A. (2009). PP2A and GSK-3beta act antagonistically to regulate active zone development. *The Journal of neuroscience : the official journal of the Society for Neuroscience* **29**, 11484-11494.

Vyas, D. R., Spangenburg, E. E., Abraha, T. W., Childs, T. E. and Booth, F. W. (2002). GSK-3beta negatively regulates skeletal myotube hypertrophy. *American journal of physiology. Cell physiology* **283**, C545-551.

Wei, J., Liu, W. and Yan, Z. (2010). Regulation of AMPA receptor trafficking and function by glycogen synthase kinase 3. *J Biol Chem* **285**, 26369-26376.

Weyhersmuller, A., Hallermann, S., Wagner, N. and Eilers, J. (2011). Rapid active zone remodeling during synaptic plasticity. *The Journal of neuroscience : the official journal of the Society for Neuroscience* **31**, 6041-6052.

Wu, H. H., Ivkovic, S., Murray, R. C., Jaramillo, S., Lyons, K. M., Johnson, J. E. and Calof, A. L. (2003). Autoregulation of neurogenesis by GDF11. *Neuron* **37**, 197-207.

Yu, X. M., Gutman, I., Mosca, T. J., Iram, T., Ozkan, E., Garcia, K. C., Luo, L. and Schuldiner, O. (2013). Plum, an immunoglobulin superfamily protein, regulates axon pruning by facilitating TGF-beta signaling. *Neuron* **78**, 456-468.

Zhang, F., Endo, S., Cleary, L. J., Eskin, A. and Byrne, J. H. (1997). Role of transforming growth factor-beta in long-term synaptic facilitation in Aplysia. *Science* **275**, 1318-1320.

MYOSTATIN-LIKE PROTEINS REGULATE SYNAPTIC FUNCTION AND NEURONAL MORPHOLOGY

Hrvoje Augustin, Kieran McGourty, Joern R. Steinert, Helena M. Cochemé, Jennifer Adcott, Melissa Cabecinha, Alec Vincent, Els F. Halff, Josef T. Kittler, Emmanuel Boucrot, Linda Partridge

MAIN FIGURES:

Figure 1. Myoglianin is a negative regulator of synaptic physiology and composition. (A) Representative samples of eEJCs recorded from muscle 6 for (B). (B) Quantification of evoked EJCs from the larvae with reduced (*Mef2-GAL4/UASmiRNAmyo*) or increased (*Mef2-GAL4/ UAS-myoglianin*) *myo* expression in muscles. Control phenotype: *+/Mef2/GAL4* (*n* = 5-9). Representative traces (C) and cumulative frequency (CF) diagram (D) of mEJC amplitudes from the larvae expressing *myo* transgenes in muscle; larger synaptic currents are indicated by a shift of the curve to the right (*n* = 6-12 animals, ~500-1200 events measured per genotype). (E and F) Representative confocal images showing the 3rd instar larval NMJ 6/7 staining for GluRIIA (E) and Brp (F). Anti-HRP labels presynaptic (motoneuronal) membrane. Scale bar: 20 µm. (G) *Left*: Quantification of GluRIIA signal intensities in larvae expressing various *myo* constructs in larval muscles (*n* = 10-18). *Right*: Number of Brp puncta normalized to the area of the 6/7 NMJ (*n* = 1215). All panels: Error bars represent SEM (ANOVA + Tukey's post-test: $^{**}p < 0.01$, $^{***}p < 0.001$ and n.s. = not significant).

Figure 2. Myoglianin is produced at the larval NMJ and is a modulator of its function. (A) Confocal images showing the NMJ expression of a GFP construct under *Myo-GAL4* control. Anti-HRP (red) marks motoneurons innervating the 6/7 NMJ; anti-GFP antibody (green) was used to enhance the GFP signal. Asterisk marks the GFP-positive area in the muscle. Inset: the arrow indicates strong GFP signal in the synaptic boutons, with the arrowheads indicating thread-like, GFP-labelled, extramuscular structures running alongside neuronal projections. Scale bar: 20 µm. Physiological measurements in larvae mis-expressing *myo* in glia: (B) Representative eEJCs traces; (C) Quantification of evoked EJCs (*n* = 5-9; ANOVA + Tukey's post-test: $^{*}p < 0.05$); (D) Representative mEJC traces; (E) Cumulative frequency diagram of mEJC amplitudes (*n* = 6-12).

Figure 3. MYO negatively regulates larval weight and muscle size. (A) Larval weights in animals with muscle-expressing *myo* constructs. (B) Wet weight in larvae with glia-manipulated *myo* expression: *repo-GAL4/UAS-miRNAmyo* (silencing), *repo-GAL4/UAS-miRNAmyo* (upregulation), *+repo-GAL4* (control). (For A and B: *n* = 1468 measurements per genotype, 3-5 larvae per measurement). (C) Part of a single larval abdominal hemisegment containing muscles 6 and 7. Scale bar: 40 µm. (D and E) Surface area of fibers 6 and 7 in denoted genotypes (*n* = 5-11). Crawling speed in 3rd instar larvae with *myo* levels manipulated in muscle (F) and glial (G) cells (*n* = 15-51). All bar graphs: Error bars indicate SEM (ANOVA + Tukey's post-test: $^{*}p < 0.05$, $^{**}p < 0.01$, $^{***}p < 0.001$ and n.s. = not significant).

Figure 4. Smad2 mediates effects of MYO on synaptic function. (A) Representative traces of evoked (top) and spontaneous (bottom) responses for indicated genotypes. (B) Activation of Smad2 in "low myo" background (*Mef2-GAL4/UAS-miRNAmyo/Smad2↑*) abolished the effect of reduced *myo*

expression on evoked response (*n* = 8-10). (C) Cumulative frequency graph showing the distribution of “mini amplitudes” in various mutants. Downregulation of *myo* caused a significant increase in the amplitude of “minis” (red line) that was completely abolished by simultaneous Smad2 activation (yellow line) (*n* = 5-15). *Mef2-GAL4/Smad2↑* flies (gray line) generated miniature amplitudes than were higher than in *+/Mef2-GAL4* controls, and significantly lower than in *Mef2-GAL4/ UAS-miRNAmyo* animals (KS test, $P < 0.0001$). (D) Wet weight measurements of third instar larvae of denoted genotypes (*n* = 13-26). For all measurements: error bars represent SEM (ANOVA + Tukey’s post-test: *$p < 0.05$, ***$p < 0.001$, n.s. = not significant).

Figure 5. Myostatin injections into developing larvae reverse the effect of *myo* downregulation in muscles. (A) Representative evoked response traces for indicated genotypes (+BSA or MST) for the quantification shown in (B). (B) Myostatin reverses the effect of *myo* down-regulation on the mean evoked EJCs in the +/*Mef2-GAL4* and *Mef2-GAL4/UAS-miRNAmyo* larvae (*n* = 5-9). Two-way ANOVA analysis: the treatment/genotype interaction is highly significant ($p = 0.0043$). (C) Myostatin negatively regulates the abundance of type II NMJ glutamate receptors in 3rd instar larvae with muscle-reduced *myo* expression. Representative confocal images for *Mef2-GAL4/UAS-miRNAmyo* larvae injected with BSA (*left*) or Myostatin (*right*). Scale bar: 30 µm. (D) Quantification of synaptic GluRIIA density in injected *Mef2-GAL4/UAS-miRNAmyo* larvae (*n* = 6-7). (E) Injection of Myostatin (maroon bars) into 2nd instar larvae (see Experimental Procedures for details) does not reverse the effect of *myo* down-regulation in muscle (*n* = 18-26) on larval weight. Two-way ANOVA analysis: the treatment/genotype interaction is ‘not significant’. All panels: Error bars indicate SEM. (ANOVA + Tukey’s post-test (A and E) or unpaired t-test (D): *$p < 0.05$, **$p < 0.01$, ***$p < 0.001$).

Figure 6. Myostatin and GDF11 modulate neurite outgrowth and synapse formation. (A) Images of rat brain isolated cortical neuron culture treated as indicated with either DMSO (Control), 5 ng/ml TGF-β1 (TGF-β), 10 ng/ml BMP2, 10 ng/ml Myostatin (also called GDF8) or 10 ng/ml GDF11 for 5 days commencing from 6 DIV. Cultures were immunostained for excitatory pre (vGLUT1, green) and post (PSD95, red) synaptic density markers in addition to a neuronal marker (MAP2, blue). Zoomed insets correspond to boxed regions and arrows indicate synapses as denoted by co-labelling with vGLUT1 and PSD95 localized to neurites (MAP2). Bars, 15 µm. **(**B) Images of rat brain cortical neuron culture treated as in (A). Cultures were immunostained for inhibitory pre (VGAT, green) and post (GPHN, red) synaptic density markers in addition to a neuronal marker (MAP2, blue). Zoomed insets correspond to boxed regions and arrows indicate synapses, as denoted by co-labelling with VGAT and GPHN localized to neurites (MAP2). Bars, 15 µm. (C) Microscopy image quantification of the median neurite area occupied per image normalised to control after indicated treatments as in (A) in addition to a TGF-β1 signalling antagonist (TGF-β inhib, 400 nM) and agonist (TGF-β bypass, 400 nM, (*n* = 3 independent experiments). (D) Microscopy image quantification of the median synapse frequency per neurite area per image normalised to control after indicated treatments as in (C). Synapses are denoted by co-labelling with vGLUT1 and PSD95 localized to neurites (MAP2) (*n* = 3 independent experiments). (E) Microscopy image quantification of the median synapse frequency per neurite area per image normalised to control after indicated treatments as in (C). Synapses are denoted by co-labelling with VGAT and GPHN localized to neurites (MAP2) (*n* = 3 independent experiments). All error bars represent mean +/-SEM. (ANOVA + Dunnett’s test: * P<0.05; ** P<0.01; *** P<0.001, n.s. = not significant).

Figure 7. Myoglianin inhibits transmission in an adult synapse. (A) Schematic diagram of the fly giant fiber system (GFS) with the indicated positions of main electrode insertion sites for electrophysiological measurements (upper stimulating electrode: stimulation of the GF cell bodies; lower stimulating electrode: motoneuronal stimulation). PSI forms cholinergic synapses with five DLMns (only 3 shown). The NMJs between TTM and DLM motoneurons and their target muscles are chemical (glutamatergic). (B) Representative traces showing latency periods (black arrow) between the stimulation and TTM depolarization. (C) Quantification of response latencies in the TTM branch of the GF circuit (*n* = 7-8). (D) TTM responses following thoracic (NMJ) stimulations (*n* = 6-7). All panels: error bars indicate SEM. (ANOVA + Tukey's post-test: *p < 0.05, **p < 0.01, ***p < 0.001, n.s. = not significant).

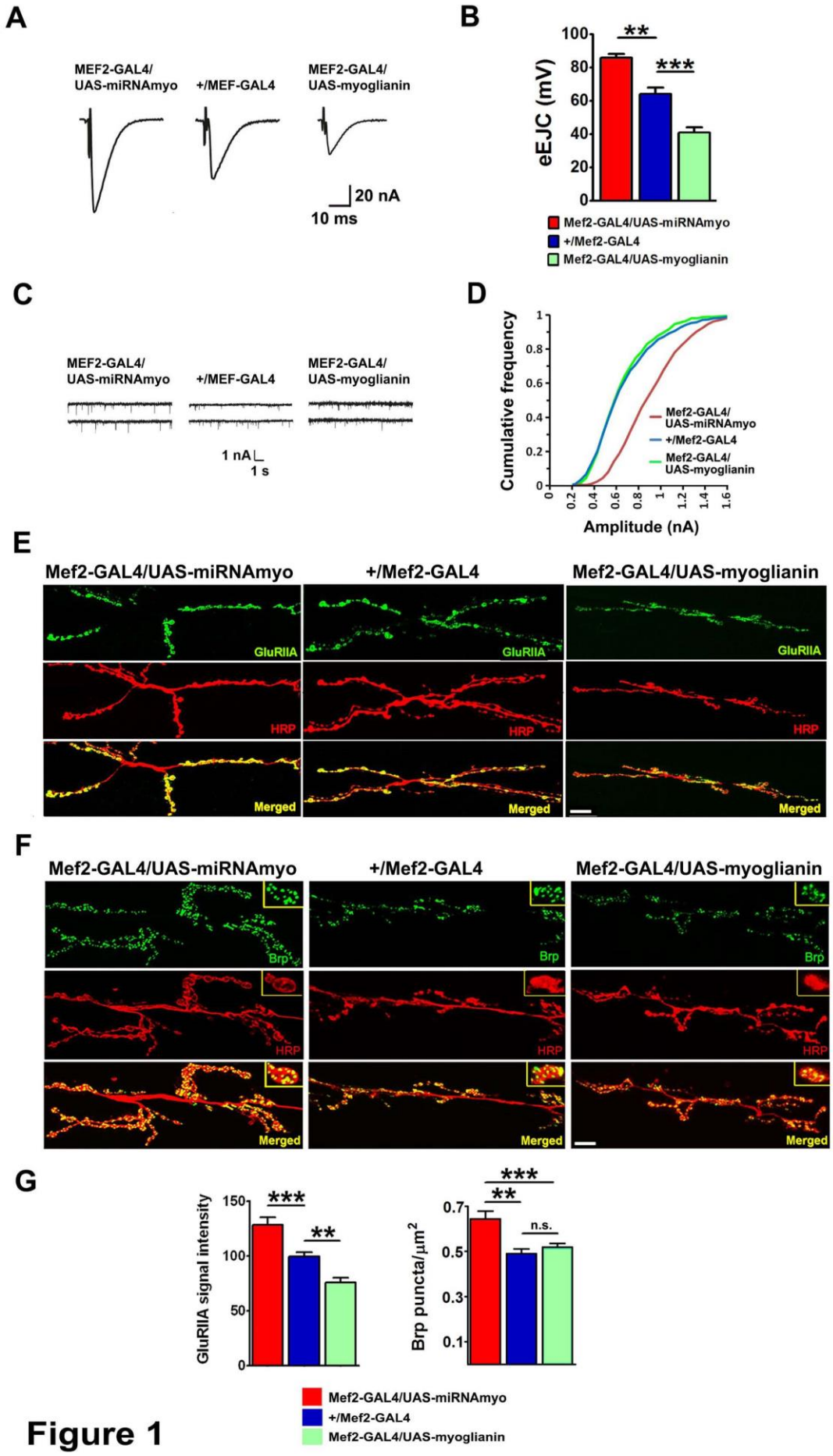
A
MEF2-GAL4/
UAS-miRNAmyo
+/MEF-GAL4
MEF2-GAL4/
UAS-myoglianin
20 nA
10 ms
B
eEJC (mV)
**
***
Mef2-GAL4/UAS-miRNAmyo
+/Mef2-GAL4
Mef2-GAL4/UAS-myoglianin
C
MEF2-GAL4/
UAS-miRNAmyo
+/MEF-GAL4
MEF2-GAL4/
UAS-myoglianin
1 nA
1 s
D
Cumulative frequency
Amplitude (nA)
Mef2-GAL4/
UAS-miRNAmyo
+/Mef2-GAL4
Mef2-GAL4/
UAS-myoglianin
E
Mef2-GAL4/UAS-miRNAmyo
+/Mef2-GAL4
Mef2-GAL4/UAS-myoglianin
GluRIIA
HRP
Merged
F
Mef2-GAL4/UAS-miRNAmyo
+/Mef2-GAL4
Mef2-GAL4/UAS-myoglianin
Brp
HRP
Merged
G
GluRIIA signal intensity
Brp puncta/μm2
***
**
n.s.
Mef2-GAL4/UAS-miRNAmyo
+/Mef2-GAL4
Mef2-GAL4/UAS-myoglianin

Figure 1

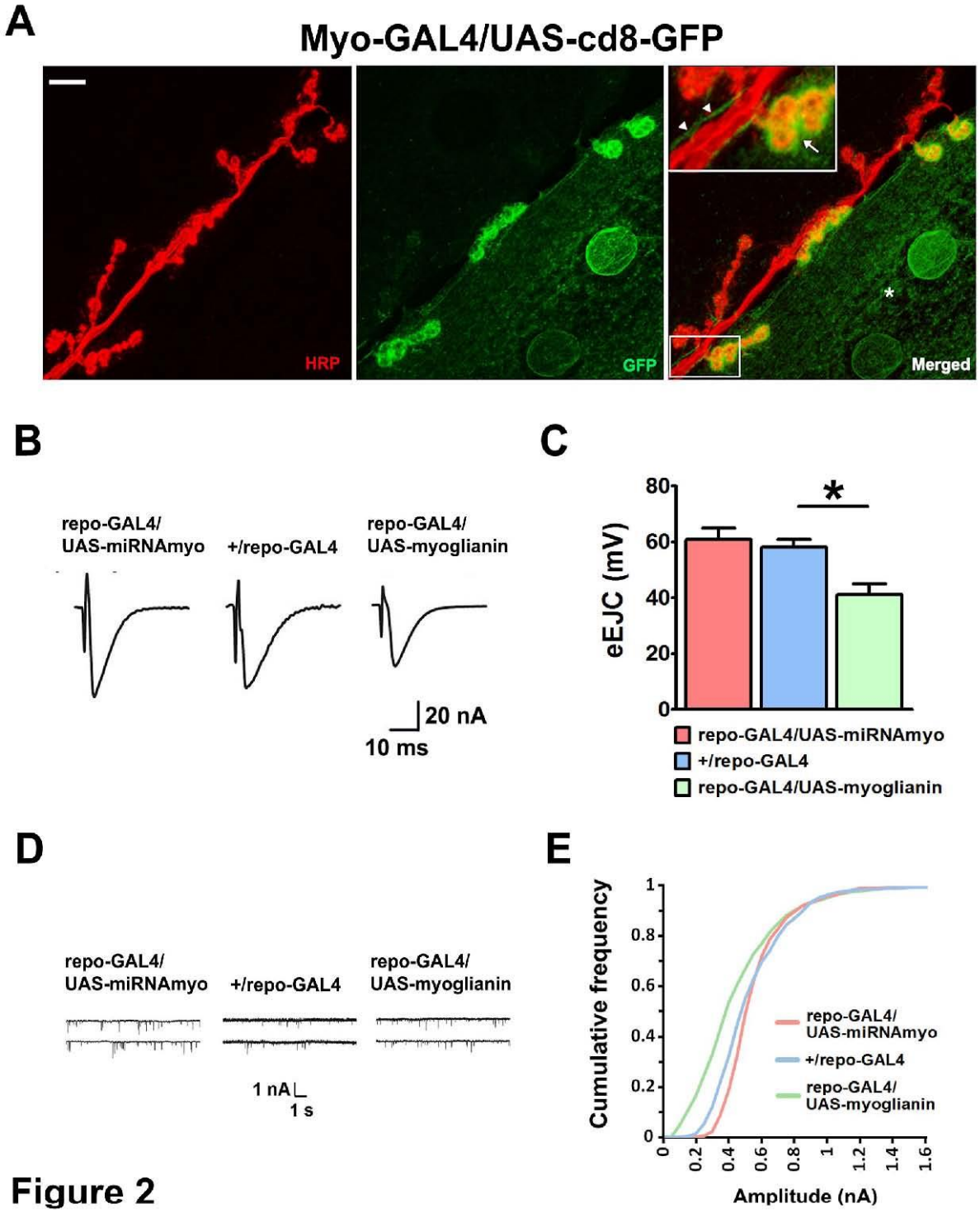
A
Myo-GAL4/UAS-cd8-GFP
HRP
GFP
Merged
B
repo-GAL4/
UAS-miRNAmyo
+/repo-GAL4
repo-GAL4/
UAS-myoglianin
20 nA
10 ms
C
eEJC (mV)
80
60
40
20
0
*
repo-GAL4/UAS-miRNAmyo
+/repo-GAL4
repo-GAL4/UAS-myoglianin
D
repo-GAL4/
UAS-miRNAmyo
+/repo-GAL4
repo-GAL4/
UAS-myoglianin
1 nA
1 s
E
Cumulative frequency
1
0.8
0.6
0.4
0.2
0
0
0.2
0.4
0.6
0.8
1
1.2
1.4
1.6
Amplitude (nA)
repo-GAL4/
UAS-miRNAmyo
+/repo-GAL4
repo-GAL4/
UAS-myoglianin

Figure 2

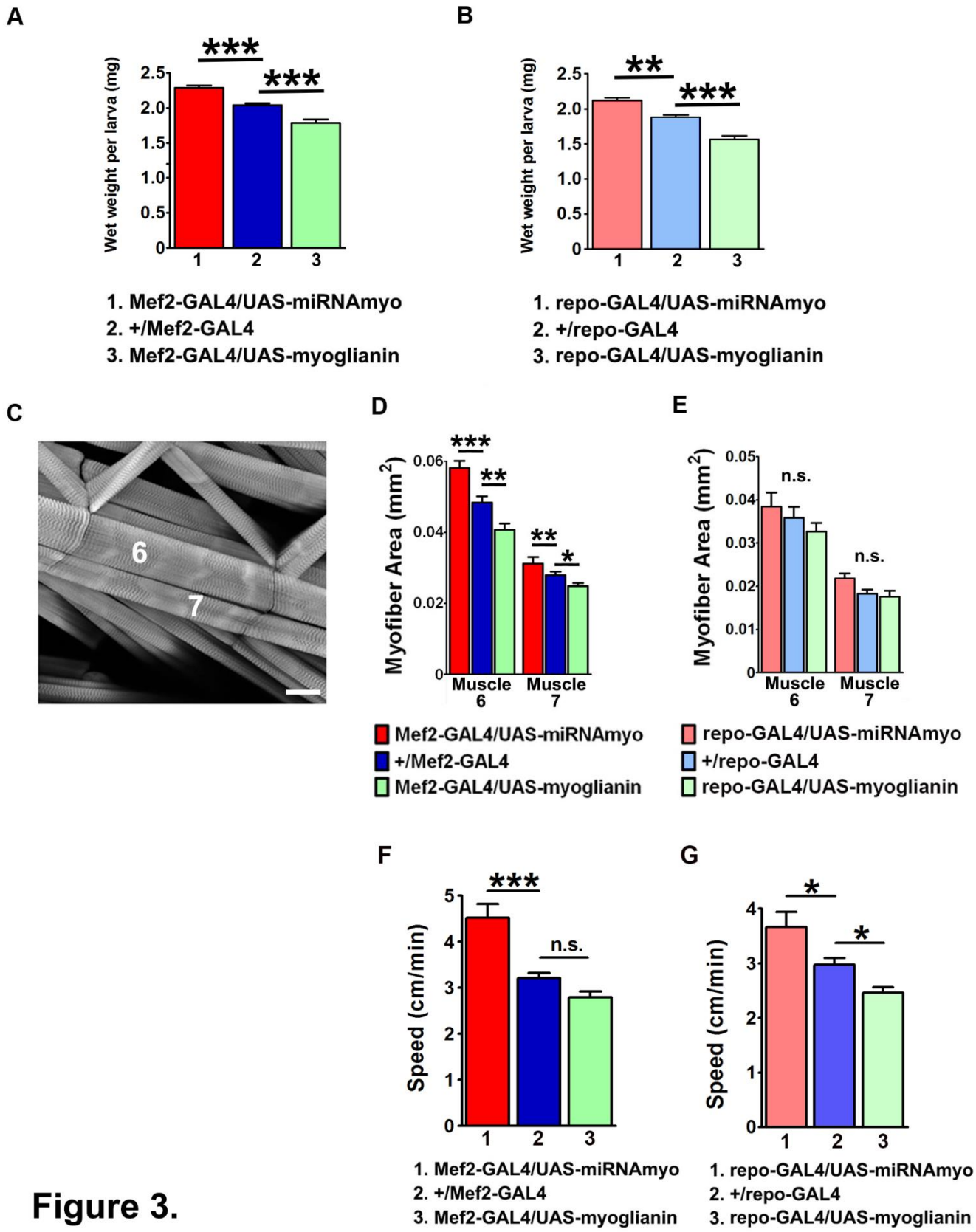
A
Wet weight per larva (mg)
***
***
1. Mef2-GAL4/UAS-miRNAmyo
2. +/Mef2-GAL4
3. Mef2-GAL4/UAS-myoglianin
B
Wet weight per larva (mg)
**
***
1. repo-GAL4/UAS-miRNAmyo
2. +/repo-GAL4
3. repo-GAL4/UAS-myoglianin
C
6
7
D
Myofiber Area (mm2)
Muscle 6
Muscle 7
Mef2-GAL4/UAS-miRNAmyo
+/Mef2-GAL4
Mef2-GAL4/UAS-myoglianin
E
Myofiber Area (mm2)
n.s.
n.s.
Muscle 6
Muscle 7
repo-GAL4/UAS-miRNAmyo
+/repo-GAL4
repo-GAL4/UAS-myoglianin
F
Speed (cm/min)
***
n.s.
1. Mef2-GAL4/UAS-miRNAmyo
2. +/Mef2-GAL4
3. Mef2-GAL4/UAS-myoglianin
G
Speed (cm/min)
*
*
1. repo-GAL4/UAS-miRNAmyo
2. +/repo-GAL4
3. repo-GAL4/UAS-myoglianin

Figure 3.

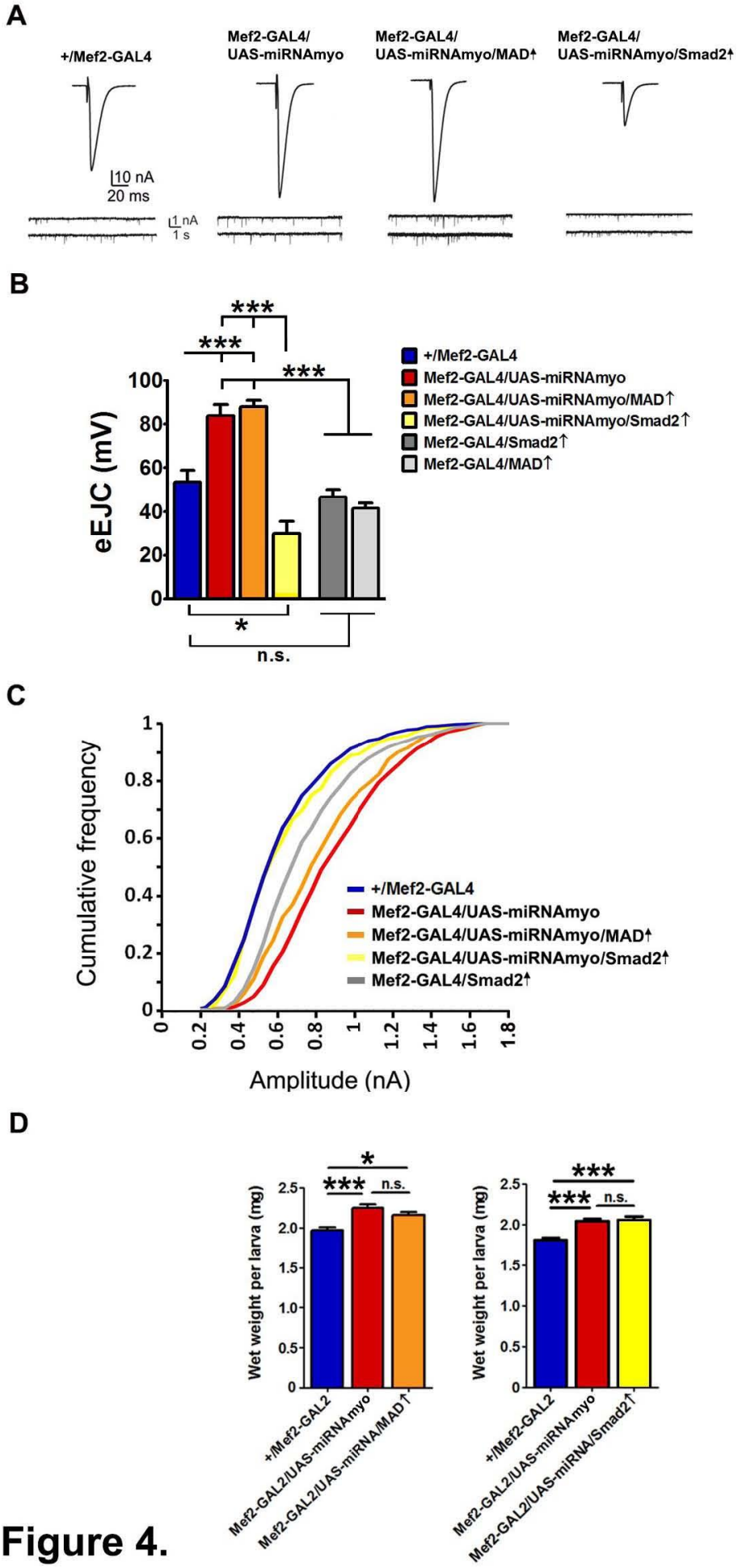
A
+/Mef2-GAL4
Mef2-GAL4/
UAS-miRNAmyo
Mef2-GAL4/
UAS-miRNAmyo/MAD↑
Mef2-GAL4/
UAS-miRNAmyo/Smad2↑
10 nA
20 ms
1 nA
1 s
B
eEJC (mV)
100
80
60
40
20
0
***
***
***
*
n.s.
+/Mef2-GAL4
Mef2-GAL4/UAS-miRNAmyo
Mef2-GAL4/UAS-miRNAmyo/MAD↑
Mef2-GAL4/UAS-miRNAmyo/Smad2↑
Mef2-GAL4/Smad2↑
Mef2-GAL4/MAD↑
C
Cumulative frequency
1
0.8
0.6
0.4
0.2
0
0
0.2
0.4
0.6
0.8
1
1.2
1.4
1.6
1.8
Amplitude (nA)
+/Mef2-GAL4
Mef2-GAL4/UAS-miRNAmyo
Mef2-GAL4/UAS-miRNAmyo/MAD↑
Mef2-GAL4/UAS-miRNAmyo/Smad2↑
Mef2-GAL4/Smad2↑
D
Wet weight per larva (mg)
2.5
2.0
1.5
1.0
0.5
0
*
***
n.s.
+/Mef2-GAL2
Mef2-GAL2/UAS-miRNAmyo
Mef2-GAL2/UAS-miRNA/MAD↑
***
***
n.s.
+/Mef2-GAL2
Mef2-GAL2/UAS-miRNAmyo
Mef2-GAL2/UAS-miRNA/Smad2↑

Figure 4.

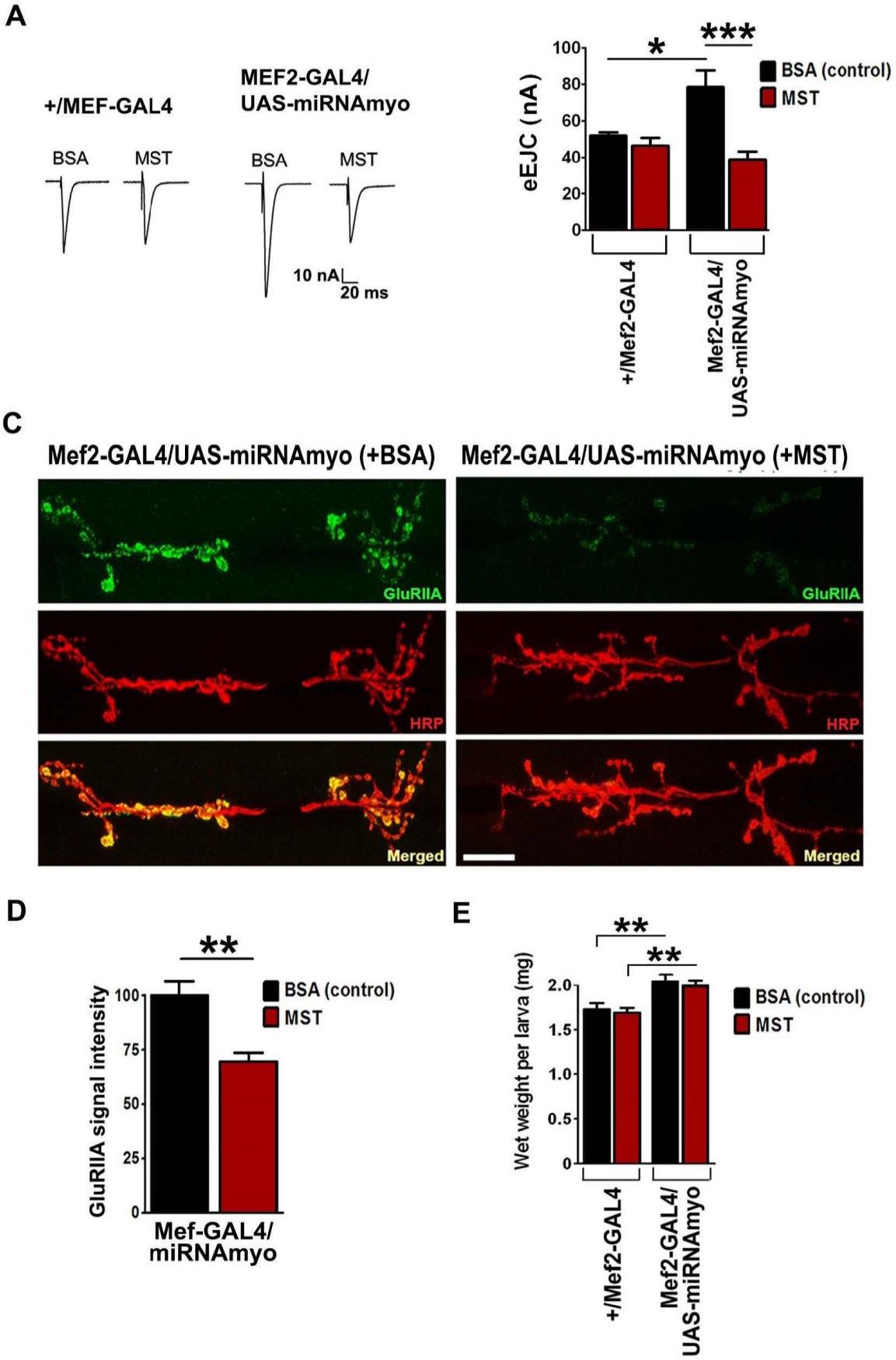
A
+/MEF-GAL4
MEF2-GAL4/
UAS-miRNAmyo
BSA
MST
BSA
MST
10 nA
20 ms
*
***
eEJC (nA)
100
80
60
40
20
0
BSA (control)
MST
+/Mef2-GAL4
Mef2-GAL4/
UAS-miRNAmyo
C
Mef2-GAL4/UAS-miRNAmyo (+BSA)
Mef2-GAL4/UAS-miRNAmyo (+MST)
GluRIIA
HRP
Merged
D
**
GluRIIA signal intensity
100
75
50
25
0
BSA (control)
MST
Mef-GAL4/
miRNAmyo
E
**
**
Wet weight per larva (mg)
2.0
1.5
1.0
0.5
0
BSA (control)
MST
+/Mef2-GAL4
Mef2-GAL4/
UAS-miRNAmyo

Figure 5.

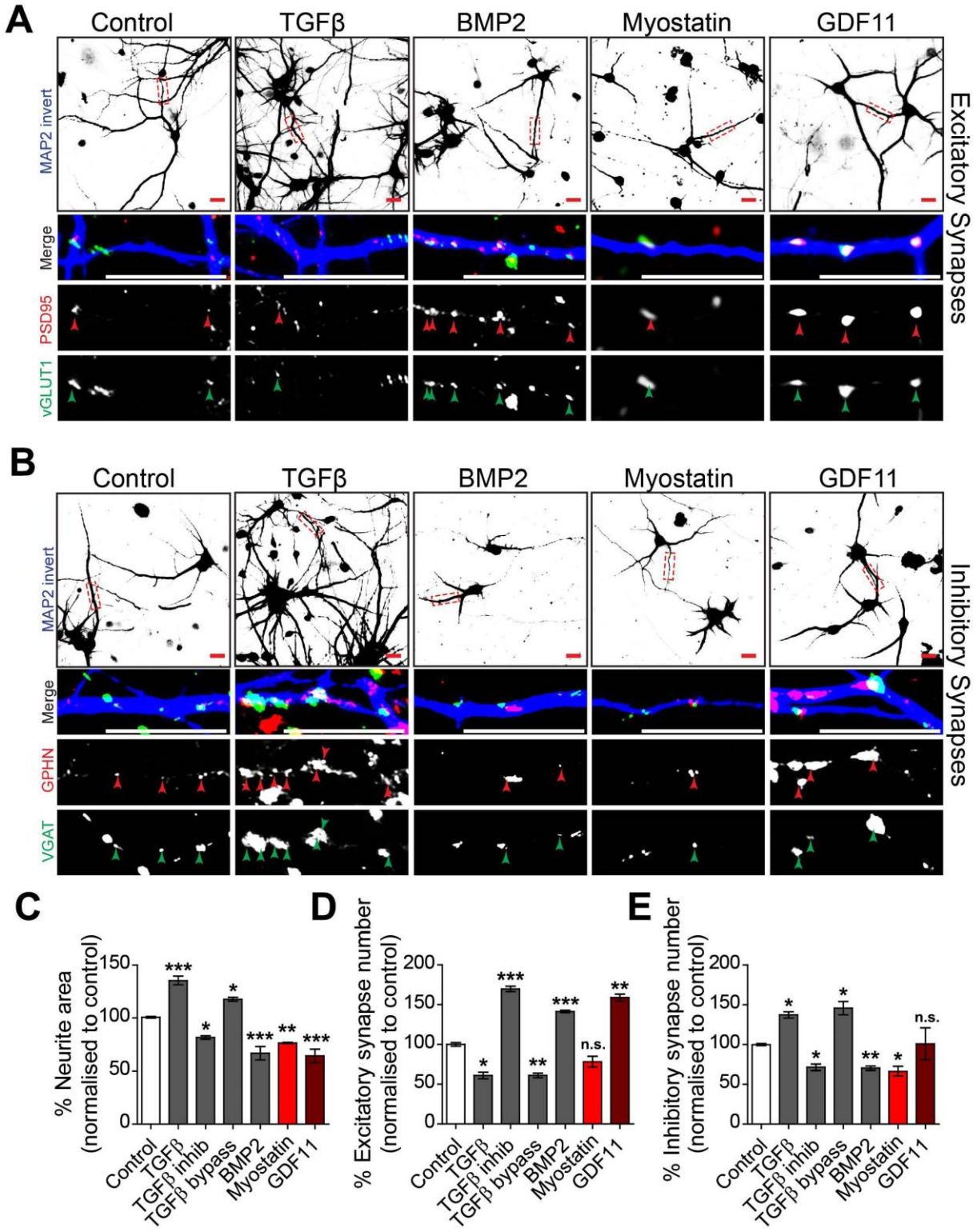
A
Control
TGFβ
BMP2
Myostatin
GDF11
MAP2 invert
Merge
PSD95
vGLUT1
Excitatory Synapses
B
Control
TGFβ
BMP2
Myostatin
GDF11
MAP2 invert
Merge
GPHN
VGAT
Inhibitory Synapses
C
% Neurite area (normalised to control)
D
% Excitatory synapse number (normalised to control)
E
% Inhibitory synapse number (normalised to control)
Control
TGFβ
TGFβ inhib
TGFβ bypass
BMP2
Myostatin
GDF11
n.s.

Figure 6.

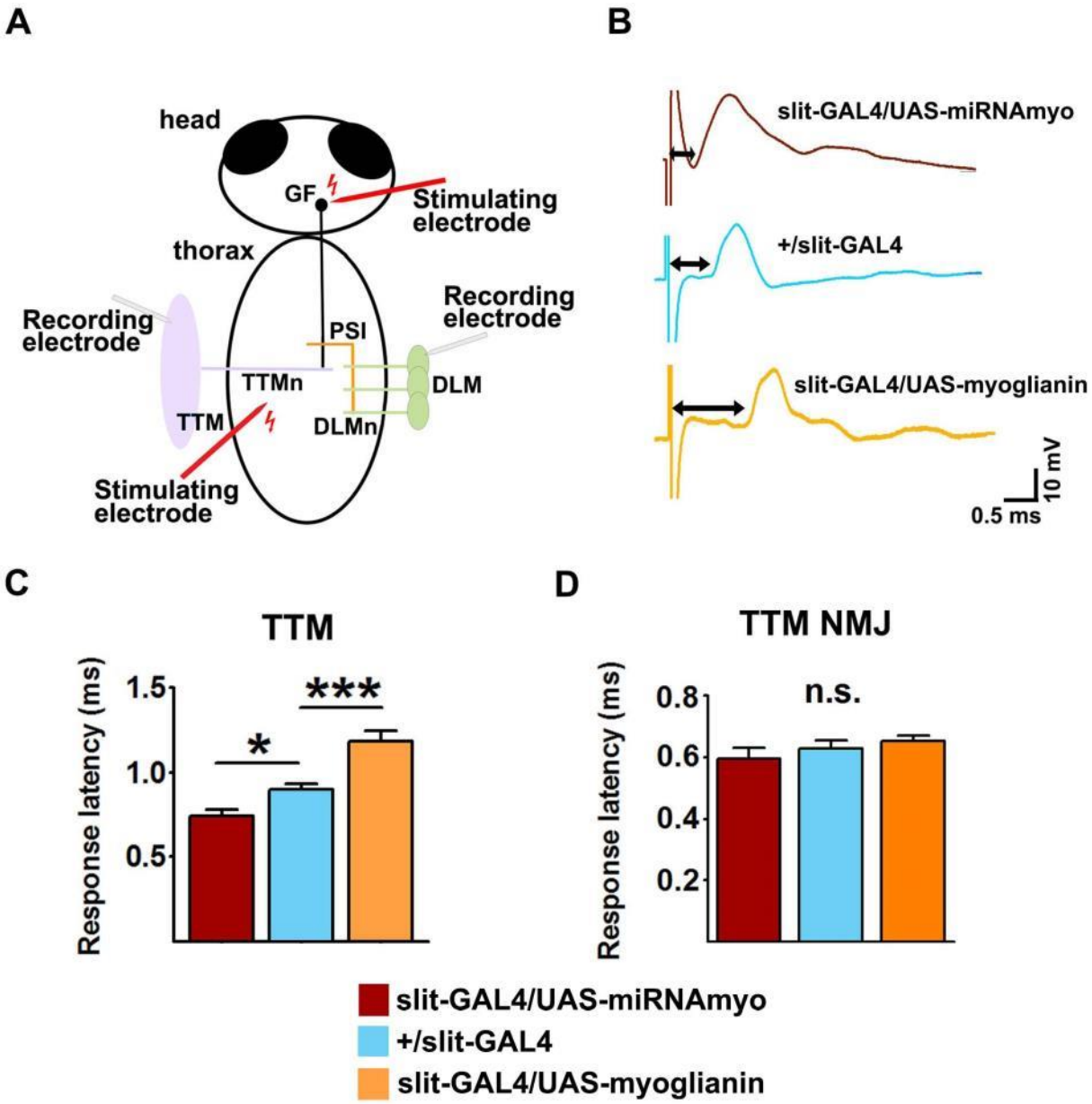
A
head
GF
Stimulating electrode
thorax
Recording electrode
Recording electrode
PSI
TTMn
DLM
TTM
DLMn
Stimulating electrode
B
slit-GAL4/UAS-miRNAmyo
+/slit-GAL4
slit-GAL4/UAS-myoglianin
10 mV
0.5 ms
C
TTM
Response latency (ms)
1.5
1.0
0.5
*
***
D
TTM NMJ
n.s.
0.8
0.6
0.4
0.2
slit-GAL4/UAS-miRNAmyo
+/slit-GAL4
slit-GAL4/UAS-myoglianin

Figure 7.